Optimization of Droop Control Coefficients in a Isolated Microgrid Cluster Using Particle Swarm Optimization

Horrillo-Quintero, Pablo; García-Triviño, Pablo; Carrasco González, David; Sarrias Mena, Raúl; García-Vázquez, Carlos Andrés; Fernández Ramírez, Luis Miguel

Published in:
2024 6th International Conference on Smart Power & Internet Energy Systems (SPIES)

DOI (link to publication from Publisher):
10.1109/SPIES63782.2024.10983545

Publication date:
2025

Document Version:
Accepted version

Citation for published version (IEEE):
P. Horrillo-Quintero, P. García-Triviño, D. Carrasco-González, R. Sarrias-Mena, C. A. García-Vázquez, and L. M. Fernández-Ramírez, “Optimization of Droop Control Coefficients in a Isolated Microgrid Cluster Using Particle Swarm Optimization,” 2024 6th International Conference on Smart Power & Internet Energy Systems (SPIES), pp. 379–384, Dec. 2024, doi: 10.1109/SPIES63782.2024.10983545.

Optimization of Droop Control Coefficients in a Isolated Microgrid Cluster Using Particle Swarm Optimization

Pablo Horrillo-Quintero
SURET Research Group
Dept.Electrical Engineering
University of Cádiz
ETSI Algeciras, Spain
pablo.horrillo@uca.es

Pablo García-Triviño
SURET Research Group
Dept.Electrical Engineering
University of Cádiz
ETSI Algeciras, Spain
pablo.garcia@uca.es

David Carrasco-González
SURET Research Group
Dept.Electrical Engineering
University of Cádiz
ETSI Algeciras, Spain
david.carrasco@uca.es

Raúl Sarrias-Mena
SURET Research Group *Dept.*
Dept.Engineering in Automation,
Elect. Comp. Arch. & Netw
University of Cádiz
ETSI Algeciras, Spain
raul.sarrias@uca.es

Carlos A. García-Vázquez
SURET Research Group
Dept.Electrical Engineering
University of Cádiz
ETSI Algeciras, Spain
carlos.garcia@uca.es

Luis M. Fernández-Ramírez
SURET Research Group
Dept.Electrical Engineering
University of Cádiz
ETSI Algeciras, Spain
luis.fernandez@uca.es

***Abstract*—The isolated operation of microgrid clusters (MGC) must ensure proper voltage and frequency control continuously, in addition to maintaining the load and establishing an efficient distribution among the microgrids (MGs). The droop control technique is the most adopted method to perform the primary control of MGs. Therefore, the optimization of the droop control coefficients is one issue that need to be addressed to achieve the optimal MGC operation. This article presents a new objective cost function aimed at minimizing the system's total operating cost while ensuring effective voltage and frequency control within the established threshold values. The particle swarm optimization (PSO) metaheuristic optimization algorithm is used to solve the optimization problem and obtain the optimal values of the droop control coefficients that guarantee MGC stability and loss minimization. An isolated MGC is implemented in the Matlab/Simulink environment. Each MG consists of a grid-supporting inverter, an inductive-capacitive filter, a power transformer, and transmission lines connecting each MG. The results obtained in different scenarios ensure effective frequency and voltage control, as well as loss minimization by applying the optimal droop coefficients obtained through PSO.**

Keywords—Microgrid cluster, isolated, droop control, PSO, loss, optimization.

I. INTRODUCTION

Microgrids (MGs) constitute an efficient technical alternative for the comprehensive management of distributed generation (DG) units, bringing generation closer to energy consumption [1]. With notable progress in MG development, the chance arises to link multiple neighboring MGs, creating a microgrid cluster (MGC) in a particular area [2–4]. In remote areas with difficult access to the main power grid, MGCs offer an efficient and interesting solution due to the possibility of sharing resources between them [5].

One of the main aspects to consider in isolated operation is the need to ensure proper voltage and frequency control without the support of a main power grid. Reduced system inertia, especially in renewable-based MGC, can lead to more rapid frequency deviations. To avoid this, it is essential to include an optimal control system. In MGC control, it is common to refer to a hierarchical structure with three levels: primary, secondary, and tertiary [6].

The primary level pertains to the operation of the system to maintain fast regulation. This is achieved through droop control and internal voltage and current loops, aiming to share the power of each DG, improve power quality, and stabilize voltage and frequency [7]. The main advantage of this layer is its quick response, as it does not need to communicate with other systems.

Nevertheless, when a disturbance, such as an increase or decrease in load, occurs in the system, the frequency and voltage will deviate from their nominal reference values. The secondary control restores the reference values of voltage and frequency that are sent to the primary control, thus ensuring the stability of the system. Compared to the primary level, it has a slower dynamic response to variations [8].

In [9], a supervised controller for unforeseen operational situations was presented. A multi-level controller with gentle, moderate, and severe actions was introduced. Mild actions

This work was partially supported by Ministerio de Ciencia e Innovación, Agencia Estatal de Investigación, FEDER, UE (Grant PID2021-123633OB-C32 supported by MCIN/AEI/10.13039/501100011033/FEDER, UE).

included adjusting the droop parameters of the sources and managing the charge/discharge of energy storage systems. The objectives set forth were the reduction of fuel usage and emissions from traditional generators, considering the connection lines between MGs, along with the deviations in frequency and voltage.

An appropriate decentralized power management strategy was proposed in [10], without a communication link between the MGs. For this purpose, one of the converters must consistently control the voltage of the DC link, and the other must function in droop control mode.

The study in [11] presented a new enhanced droop regulation method is suggested utilizing a multi-objective evolutionary metaheuristic technique known as the centripetal force gravity search algorithm, aiming to improve the efficacy of droop in energy distribution, with the objectives of improving supply quality and maintaining demand.

The conventional active power droop regulator (see Eq. (1)) distributes active energy across DG units according to their capacity proportions. Nevertheless, this approach to power distribution does not ensure cost-effective functionality of the system. Rather than employing Eq. (1), this paper introduces an optimal active power droop control strategy that allocates active energy among DG units, thereby minimizing the total generation expenses of the system [12].

This paper presents a comprehensive approach to the adaptive optimization of droop control coefficients based on load to ensure voltage and frequency control in an isolated MGC. It takes into account the losses in the lines that interconnect the MGs, as well as the filters and power transformers of the isolated MGC, to minimize total operating costs based on the particle swarm optimization (PSO) algorithm. The cost function to be optimized considers the generation costs of two DGs and the costs associated with the total losses of the MGC, demonstrating that this function depends exclusively on the droop control coefficients, the measured frequency, and the established maximum frequency value for control.

The rest of this article is structured as follows: Section II presents the configuration of the isolated MGC under study, Section III describes the control scheme and the proposed PSO optimization algorithm. Section IV illustrates and discusses the results of the simulations conducted in Matlab/Simulink. Finally, the conclusions derived from this study are outlined in Section V.

II. MICROGRID CLUSTER CONFIGURATION

Fig. 1 shows a diagram of the proposed MGC. The configuration consists of two MGs connected in parallel to the point of common coupling (PCC) through grid-supporting inverters. The rated power of both inverters is 500 kW. These inverters are responsible for maintaining voltage and frequency and performing optimal power dispatch between the MGs. A transmission line links the local loads to the converters, which have an inductance and loss resistance.

Each MG comprises a two-level three-phase power converter, a LC filter, a 480/600V power transformer, as well as a DC source to represent the DC link of a typical MG with distributed energy resources.

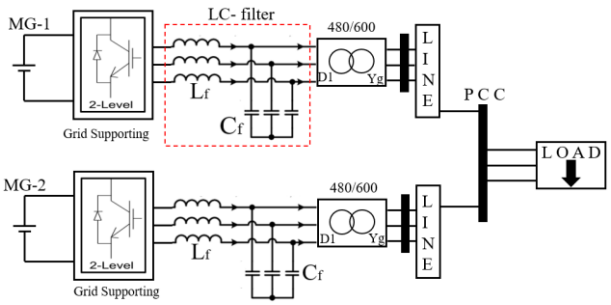

Fig. 1. Isolated MGC configuration.

III. MGC CONTROL ARCHITECTURE

A. Control System

This section provides a detailed description of the control scheme for the MGC, which is based on an optimized version of primary control based on droop control method. Furthermore, it includes a secondary control of frequency and voltage. Fig. 2 shows the proposed control scheme.

Based on Eq. (1), the frequency of each MG can be expressed as follows (Fig. 2a).

$$f_i = f_{o,i} + n_{,i}(P_{o,i} - P_i) \quad (1)$$

where f_i denotes the measured frequency of each MG, $f_{o,i}$is the reference frequency, n_i is the frequency droop control coefficient, $P_{o,i}$ is the power at the frequency $f_{o,i}$ and P_i is the measured active power. It is important to note that the subscript i (1,2) corresponds to each respective MG.

In a similar analysis, the output voltage of each MG is obtained from the following expression.

$$V_i = V_{o,i} - m_i Q_i \quad (2)$$

where V_i represents the output voltage, $V_{o,i}$ is the reference voltage, m_i is the voltage droop control coefficient and Q_i is the measured reactive power. Note that for the voltage droop control, it is assumed that $Q_{o,i}$ is zero.

Once the value of f_i is obtained, the value of the term wt is computed, which is necessary to convert the sinusoidal measurements of current and voltage (I_{abc}, V_{abc}) into the direct-quadratic coordinate frame, that is, $V_d^*, V_q^*$and I_d^*, I_q^*. This will facilitate the implementation of PI controllers. The subscript 'd' refers to the direct component, while the subscript 'q' refers to the quadrature component. Note that the superscript * denotes the reference values.

Voltage control (Fig. 2b) is responsible for adjusting the measured values of V_d, V_q to the desired values, which are derived from Eq. (2). To achieve this, a PI controller adjusts the error between V_d, V_q and V_d^*, V_q^*. The output signal of each PI controller will thus be the reference current values for each converter, that is, I_d^*, I_q^*.

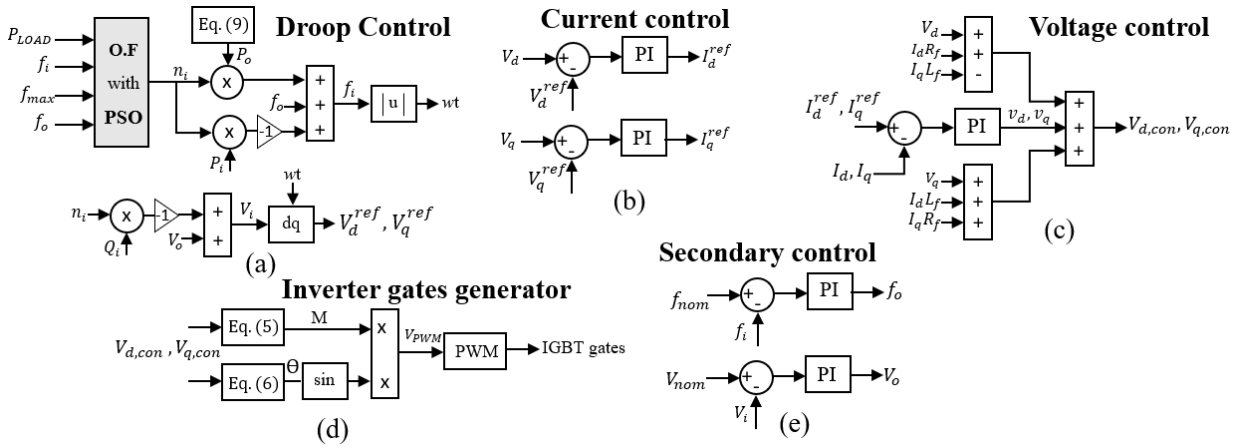

Fig. 2. MGC control scheme: (a) Optimized PSO droop control, (b) current control, (c) voltage control, (d) inverter gates generator voltage, and (e) secondary control

Current control (Fig. 2c) aims to adjust the measured values of I_d, I_q to the previously obtained reference values. Similarly, a PI controller is employed to adjust the error between I_d, I_q and I_d^*, I_q^*. The outputs of these PI controllers are denoted as $v_{d,i}$ and $v_{q,i}$, which are the voltage values that each grid-supporting inverter must control. Since the 'd' and 'q' components are not completely independent, it is necessary to decouple the 'd' and 'q' axes. To achieve this, feedforward decoupling is used to compute the direct and quadrature control components of the converter ($V_{d,con}, V_{q,con}$) according to the following expressions.

$$V_{d,con} = V_d + I_d R_f - I_q L_f + v_{d,i} \quad (3)$$

$$V_{q,con} = V_d + I_d L_f + I_q R_f + v_{q,i} \quad (4)$$

where R_f and L_f denote the resistance and inductance of the filter.

The pulses for each inverter are generated using a classic pulse width modulation (PWM) technique. The magnitude of the modulation index (M) is obtained from Eq. (5):

$$\mathrm{M} = \left| \frac{\mathrm{V_{d,con}}, \mathrm{V_{q,con}}}{\frac{\mathrm{V_{DC}}}{2} \frac{1}{\frac{\mathrm{V_{sec}^* \sqrt{2}}}{\sqrt{3}}}} \right| \quad (5)$$

$$\Theta = \angle \left(\frac{V_{d,con}, V_{q,con}}{\frac{V_{DC}}{2} \frac{1}{\frac{V_{sec}^* \sqrt{2}}{\sqrt{3}}}} \right) + wt \quad (6)$$

The control voltage (V_{PWM}) is obtained by combining the value of M with the phase angle, according to

$$\mathrm{V_{PWM}} = \mathrm{M} \sin \Theta \quad (7)$$

where Θ denotes the phase of V_{PWM}, V_{DC} is the input direct voltage and V_{sec}^* is the nominal secondary voltage of the transformer.

The PWM block is responsible for generating the triggering pulses for the grid-supporting IGBTs of the inverter, thereby controlling the voltage and frequency according to the optimized droop control strategy described (Fig. 2d).

Finally, the secondary control (Fig. 2e) is responsible for restoring the values of f_i, V_i, since the primary control does not ensure that they can be maintained according to the reference values. To achieve this, the value of f_o is obtained as the output of a PI controller that adjusts the error between the measured frequency (f_i) and the nominal frequency of the MGC (f_{nom}). Similarly, the value of V_o is computed as the output of another independent PI controller that adjusts the error between the measured voltage (V_i) and the nominal voltage of the MGC (V_{nom}).

B. Optimization of Droop Control Coefficients based on PSO

This paper aims to minimize the overall operating costs of the MGC. To this end, it takes into account the total losses of the system and the generation costs associated with each MG, in accordance with

$$OF = \min \left(\sum C_i P_i + \sum C_{LOS,i} P_{LOS,i} \right) \quad (8)$$

where C_i denotes the operating cost of each DG, C_{LOS} is the cost associated of the losses and P_{LOS} are the total losses of the MGC, considering the losses in the transmission lines, the filters and the power transformer.

According to Eq. (1), the power of each MG is a function of the droop coefficient and the system frequency. From this, it is possible to express the term $P_{o,i}$ as

$$P_{o,i} = P_{f,max} + \frac{f_{max} - f_{nom}}{n_i} \quad (9)$$

where $P_{f,max}$ is the power at maximum frequency, and f_{max} is the maximum frequency allowed.

Setting $P_{f,max}$ equal to 0 and $f_{nom} = 1$ pu, it is possible to express P_i by specifying Eq. (1) and Eq. (9) as

$$P_i = \frac{f_{max} - 1 + f_{o,i} - f_i}{n_i} \tag{10}$$

The power associated with the losses of each MG ($P_{LOS,i}$) can be expressed as

$$P_{LOS,i} = 3I_i^2 R_i \tag{11}$$

where I_i is the current of each MG, and R_i denotes the equivalent resistance losses of each MG.

The next step is to express $P_{LOS,i}$ as a function of P_i. This can be achieved using the following expression:

$$I_i = \frac{P_i}{\sqrt{3} V_i cos_{\varphi i}} \tag{12}$$

where $cos_{\varphi i}$ is the power factor, the cosine of the angle between V_i y I_i (rms values).

By combining Eqs. (10), (11), and (12), it is possible to express Eq. (8) as a function of the values of f and n_i. For the case of the MGC proposed in Section II, the following expression is obtained

$$\begin{aligned} OF = {} & C_1 \left(\frac{f_{max} - 1 + f_{o,1} - f_1}{n_1} \right) \\ & + C_2 \left(\frac{f_{max} - 1 + f_{o,2} - f_2}{n_2} \right) \\ & + C_{LOS,1} \left(3 \left(\left(\frac{f_{max} - 1 + f_{o,1} - f_1}{n_1 \sqrt{3} V_1 cos_{\varphi 1}} \right)^2 \right) R_1 \right) \\ & + C_{LOS,2} \left(3 \left(\left(\frac{f_{max} - 1 + f_{o,2} - f_2}{n_2 \sqrt{3} V_2 cos_{\varphi 2}} \right)^2 \right) R_2 \right) \end{aligned} \tag{13}$$

Consequently, the proposed objective function solely relies on the droop control coefficients and frequency. By optimizing these coefficients, energy losses (represented by the third and fourth terms) can be effectively reduced, thereby lowering operating costs in an isolated MGC.

To solve the optimization problem, the PSO metaheuristic technique is employed. PSO is chosen for its easy implementation and low computational cost. It is effective in handling nonlinear and multidimensional problems, converging quickly to optimal solutions. Its population-based approach provides robust global search capabilities, reducing the likelihood of getting trapped in local minimum[13].

The PSO optimization function has been implemented in Matlab using the particle swarm solver with the following constraints:

$$\begin{aligned} n_i &\in [lb, ub] \\ P_1 + P_2 &= P_{LOAD} + P_{LOS,1} + P_{LOS,2} \end{aligned} \tag{14}$$

The first constraint limits the possible values of the droop control coefficients to restrict the maximum allowable deviation in frequency and voltage control. On the other hand, the second constraint ensures power balance within the MGC, such that the power generated by each MG must equal the load and the total losses of the MGC.

The PSO formulation is given as

$$\mathrm{x}\,(\mathrm{k}+1) = \mathrm{x}(\mathrm{k}) + \mathrm{v}(\mathrm{k}+1) \tag{15}$$

$$\mathrm{v}(\mathrm{k}+1) = \mathrm{w}\mathrm{v}^k + r_1 c_1 ({x_{pbest}}^k - \mathrm{x}^k) + r_1 c_1 ({x_{pbest}}^k - \mathrm{x}^k) \tag{16}$$

where x denotes the position of each particle at an instant k, v denotes the velocity of each particle, w is the inertia factor, r_i are stochastic random coefficients between 0 and 1, c_i are acceleration coefficients, and x_{pbest} is the best position of the particle up to the current iteration. Note that the superscript k refers to each iteration.

IV. Results and Discussion

This section presents the simulations conducted in MATLAB/Simulink to verify the control of the isolated MGC and demonstrate the validity of the PSO algorithm in optimizing the droop control coefficients to minimize operating costs and reduce losses in the MGC. Table I summarizes the parameters of the MGC.

Fig. 3 illustrates the proposed case study in this section. The measured active power profile at the PCC (P_{PCC}) corresponds to a load variation of 300 kW for the first 10 seconds, 400 kW for the next 10 seconds, 500 kW for the following 10 seconds, and finally, decreasing to 200 kW for the last 10 seconds of simulation. It is enforced that the reactive power (Q_{PCC}) remains at zero throughout all scenarios. The optimal values of the droop coefficients are shown in Table II for each load scenario. The performance of the optimal values from the PSO algorithm is compared to a set of random values of n_i that must also satisfy Eq. (14).

TABLE I. MGC PARAMETERS.

Symbol	Parameter	Unit
V_{nom}	Rated voltage	600 V
f_{nom}	Rated frequency	60 Hz
L_f	Filter inductance	1.08 mH
R_f	Filter resistance	1.08 mΩ
C	Filter capacitance	184 µF
Z_{LINE}	Transmission line	5 mΩ +1 mH

TABLE II. PSO DROOP OPTIMAL COEFFICIENTS.

Load	n_1 (%)	n_2 (%)
300 kW	3.4906	3.1770
400 kW	4.5707	1.7127
500 kW	1.5996	2.6420
200 kW	5	5

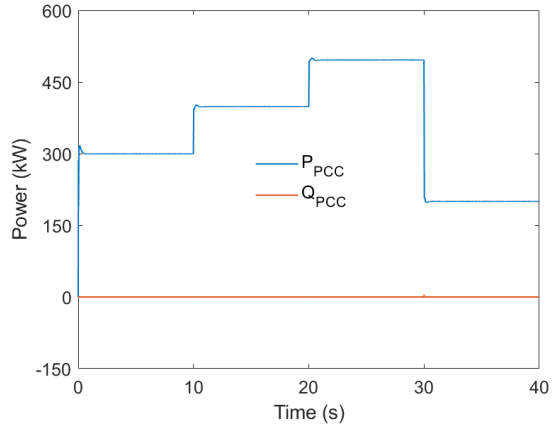

Fig. 3. Active power and reactive power measured at PCC.

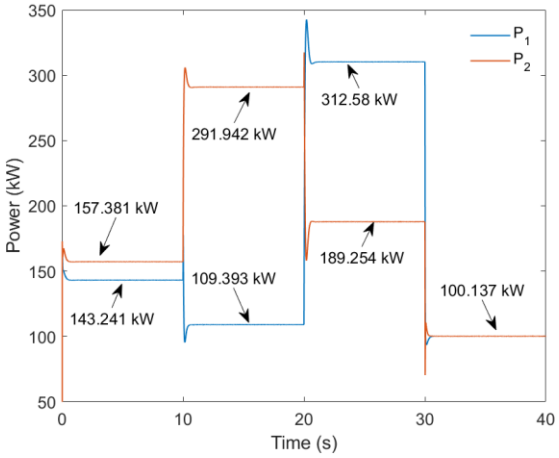

Fig. 4. MGs optimal generation power.

Fig. 4 shows the active power values for each MG. During the first 10 seconds, P_1 delivers a power of 143.241 Kw, while P_2 is at 157.381 kW, ensuring a total of 300 kW for the load. For this scenario, the total losses are 622 W, while for the benchmark they are 780 W, representing a 20% reduction. For the second load level of 400 kW, P_1 delivers 109.393 kW and P_2 delivers 291.942 kW, resulting in total losses of 1335 W. In the reference case, the loss values amount to 1.381 kW, indicating an increase of 3.4%.

The third scenario represents the highest load considered at 500 kW. In this case, P_1 contributes 312.58 kW while P_2 injects 189.254 kW. The losses in the MGC therefore amount to 1834 W, decreasing by 16.14% compared to the reference case, which is at 2130 W. Finally, the minimum load of 200 kW is equally distributed between the two MGs since they have the same droop coefficient. Both MGs inject a value of 100.137 kW, resulting in losses of 275 W. For the reference case, the losses in the last scenario are 347 W, representing an increase of 26.19%.

In Fig. 5, the loss values associated with each MG are represented, namely $P_{LOS,1}$ and $P_{LOS,2}$. The values of P_{OPT}, which is the sum of $P_{LOS,1}$ and $P_{LOS,2}$, are also shown. Finally,

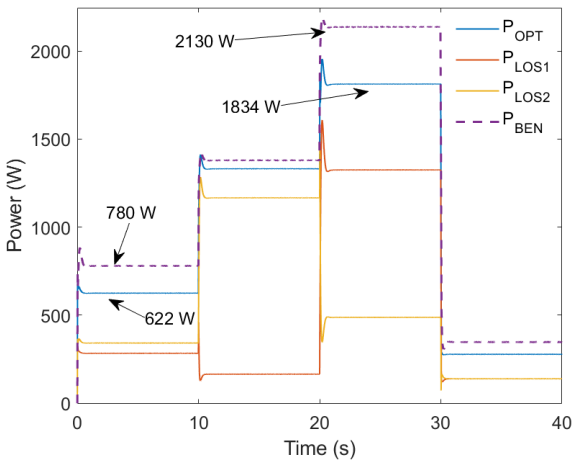

Fig. 5. MGC optimal losses and benchmark losses.

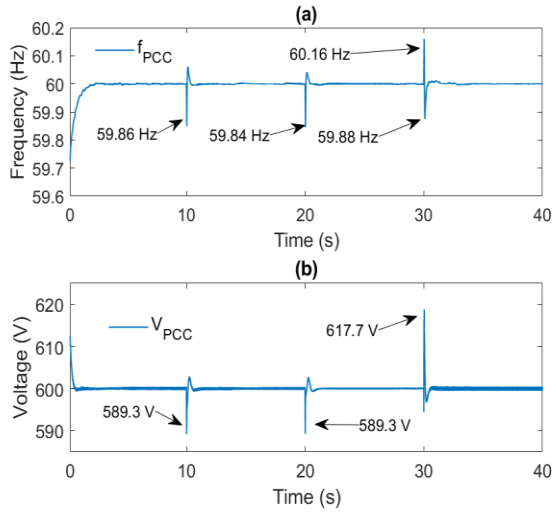

Fig. 6. PCC measures: (a) frequency control, and (b) voltage control.

the loss values for the benchmark case (P_{BEN}) are included. It is demonstrated that, for all the cases studied, the PSO algorithm shows greater optimization of the powers of each MG, minimizing the total losses.

The frequency and voltage control of the MGC are represented in Fig. 6a and Fig. 6b, respectively. The nominal frequency of the MGC is 60 Hz. The maximum allowable frequency is set at 60.3 Hz, and the minimum at 59.7 Hz, corresponding to a droop slope of 1% for frequency control. During the first scenario, from 0 to 10 seconds, the frequency is effectively maintained at 60 Hz. When the system load changes from 300 to 400 kW at 20 seconds, a frequency change is observed, reaching 59.86 Hz, which is within the allowed range. When the load increases again from 400 to 500 kW at 30 seconds, the frequency of the MGC decreases once more. In this case, the frequency drops to 59.88 Hz, remaining within the permitted threshold. Finally, when the load decreases from 500 to 200 kW at 30 seconds, the frequency increases to 60.16 Hz, which is below the maximum of 60.3 Hz. Therefore, the

effectiveness of the proposed control system in managing frequency is demonstrated.

For the voltage control, the nominal value of the MGC is 600 V. The maximum allowable voltage is set at 624 V, and the minimum at 576 V, corresponding to a droop slope of 4% for voltage control. When the load increases at 10 seconds, the voltage drops to 589.3 V, which is within the permitted threshold. Similarly, the voltage drops again to 589.3 V at 20 seconds when the load is increased to 500 kW. Finally, the maximum voltage value is reached at 30 seconds, measuring 617.7 V. This demonstrates the effectiveness of the control system in maintaining voltage within the allowed thresholds and minimizing losses in the MGC.

V. CONCLUSIONS

This article has presented the optimal operation of an isolated MGC based on grid-supporting inverters. A new objective cost function was introduced that accounts for the total operating costs of the MGC, including total losses. It has been demonstrated that to optimize this cost function, it is possible to derive an expression that depends solely on the droop control coefficients and the system frequency. By applying the PSO metaheuristic algorithm, the droop control coefficients that minimize the total losses of the system while satisfying the demand were obtained. The proposed control system effectively maintains frequency and voltage levels within according to the allowed threshold values, incorporating the optimal droop control coefficients in its operation. Different simulation scenarios have shown the superiority of the proposed PSO algorithm compared to a benchmark case in reducing the total losses of the MGC.

REFERENCES

[1] Uddin M, Mo H, Dong D, Elsawah S, Zhu J, Guerrero JM. Microgrids: A review, outstanding issues and future trends. Energy StrategyReviews2023;49. https://doi.org/10.1016/j.esr.2023.101127.

[2] Bordbari MJ, Nasiri F. Networked Microgrids: A Review on Configuration, Operation, and Control Strategies. Energies (Basel) 2024;17. https://doi.org/10.3390/en17030715.

[3] de la Cruz J, Wu Y, Candelo-Becerra JE, Vásquez JC, Guerrero JM. Review of Networked Microgrid Protection: Architectures, Challenges, Solutions, and Future Trends. CSEE Journal of Power and Energy Systems 2024;10:448–67. https://doi.org/10.17775/CSEEJPES.2022.07980.

[4] Bandeiras F, Pinheiro E, Gomes M, Coelho P, Fernandes J. Review of the cooperation and operation of microgrid clusters. Renewable and Sustainable Energy Reviews 2020;133. https://doi.org/10.1016/j.rser.2020.110311.

[5] Qazi HS, Zhao T, Liu N, Wang T, Ullah Z. Optimal Operation of Isolated Micro-Grids-cluster Via Coalitional Energy Scheduling and Reserve Sharing. Front Energy Res 2021;9. https://doi.org/10.3389/fenrg.2021.629131.

[6] Mbungu NT, Ismail AA, AlShabi M, Bansal RC, Elnady A, Hamid AK. Control and estimation techniques applied to smart microgrids: A review. Renewable and Sustainable Energy Reviews 2023;179. https://doi.org/10.1016/j.rser.2023.113251.

[7] Issa W, Sharkh S, Abusara M. A review of recent control techniques of drooped inverter-based AC microgrids. Energy Sci Eng 2024;12:1792–814. https://doi.org/10.1002/ese3.1670.

[8] Sainz L, Fernández-Ramírez LM, Jurado F, Horrillo-Quintero P. Overview of Challenges of Microgrid Clusters. Proceedings of the IEEE International Conference on Industrial Technology, Institute of Electrical and Electronics Engineers Inc.; 2024. https://doi.org/10.1109/ICIT58233.2024.10540682.

[9] Batool M, Shahnia F, Islam SM. Multi-level supervisory emergency control for operation of remote area microgrid clusters. Journal of Modern Power Systems and Clean Energy 2019;7:1210–28. https://doi.org/10.1007/s40565-018-0481-6.

[10] Ferdous SM, Shahnia F, Shafiullah GM. Power sharing and control strategy for provisionally coupled microgrid clusters through an isolated power exchange network. Energies (Basel) 2021;14. https://doi.org/10.3390/en14227514.

[11] Taha MQ, Kurnaz S. Droop Control Optimization for Improved Power Sharing in AC Islanded Microgrids Based on Centripetal Force Gravity Search Algorithm. Energies (Basel) 2023;16. https://doi.org/10.3390/en16247953.

[12] Ghosh, Arindam & Zare, Firuz (2023) Control of power electronic converters with microgrid applications. IEEE Press Series on Power and Energy Systems. John Wiley & Sons, Hoboken, NJ.

[13] Papazoglou G, Biskas P. Review and Comparison of Genetic Algorithm and Particle Swarm Optimization in the Optimal Power Flow Problem. Energies (Basel) 2023;16. https://doi.org/10.3390/en16031152.

Authors' background

Name	Prefix	Research Field	Email	Personal website
Pablo Horrillo-Quintero	PhD Candidate	Electrical Engineering	pablo.horrillo@uca.es	https://tep023.uca.es/
Pablo García-Triviño	Associate Professor	Elecrical Engineering	pablo.garcia@uca.es	https://tep023.uca.es/
David Carrasco-González	PhD Candidate	Electrical Engineering	david.carrasco@uca.es	https://tep023.uca.es/
Raúl Sarrias-Mena	Associate Professor	Electrical Engineering	raul.sarrias@uca.es	https://tep023.uca.es/
Carlos A. García-Vázquez	Associate Professor	Electrical Engineering	carlos.garcia@uca.es	https://tep023.uca.es/
Luis M. Fernández-Ramírez	Full Professor	Electrical Engineering	luis.fernandez@uca.es	https://tep023.uca.es/